# Influence of Temperature on Mineral Evolution of Cocoa Pod Husk Ash

**B.J. Olawuyi[1]; C.C. Uzoma[2,], I. O. Omuh[3], N.B. Iheama[4]**

**[1]Dept. of Building Technology, College of Science and Technology, Covenant University, Ota & Dept. of Building, School of Environmental Technology, Federal University of Technology, Minna**

**[2,3]Dept. of Building Technology, College of Science and Technology, Covenant University, Ota**

**[4]Department of Building, Faculty of Environmental Sciences, Nnamdi Azikiwe University, Awka**

**DOI: https://doi.org/10.51244/IJRSI.2026.1308000035**

**Received: 09 August 2026; Accepted: 17 August 2026; Published: 29 August 2026**

## ABSTRACT

The transformation of agricultural residues into value-added materials is critical for sustainable development in low-income regions. This study investigates the mineral oxide evolution of Cocoa Pod Husk Ash (CPHA) subjected to thermal treatment at temperatures ranging from 500 °C to 800 °C at 50 °C step intervals. The resulting Cocoa Pod Husk Ash (CPHA) from the thermal treatment were tested using the X-ray fluorescent (XRF) and Fourier Transmission Infra-Red (FTIR) analysis for an examination of the influence of temperature on the oxide composition, physical characteristics, and subsequent application potential. The XRF results revealed CaO as the major oxide in CPHA, having its highest concentrations of 53.4% at 600 °C and 51.03% at 650 °C. The $SiO_2$ content also varied as the burning temperature changes with a peak value of 20.6% at 650 °C. The FTIR indicated varied compound phases as the burning temperature differs with an inference that the 600 - 650 °C temperature is the best for good amorphous properties and that CPHA will be better used in conjunction with another reactive Pozzolan of high $SiO_2$ content for good performance as a supplementary cementitious material.

**Keywords:** Cocoa pod husk ash, calcination, mineral oxides, pozzolanic materials, sustainable construction.

## INTRODUCTION

Sustainability is a global priority; eco-friendly construction material has become very important. Due to huge urbanization activities, a lot of environmental issues are originating. Building construction using sustainable materials will lead to as well as improve the existing situation of environmental problems (Kumar and Kapur, 2025). The need for sustainable cost-effective building materials has prompted increased research into agricultural by-products and waste (Oyebisi, Igba, and Oniyide, 2019; Awoyera and Ugwu, 2022; Balador, 2024; Chen et al., 2024; Sarangi and Suganya, 2024; Parlato, Valenti, Guerrini, Perbellini, and Pezzuolo, 2025). Cocoa Pod Husk (CPH), a waste product of cocoa production, is abundant in countries such as Nigeria, Ghana, the Ivory Coast, and other West African countries. When thermally treated, CPH can yield ash rich in reactive oxides such as silica ($SiO_2$), iron oxide ($Fe_2O_3$), and calcium oxide (CaO), making it a potential candidate for use as supplementary cementitious materials (SCMs) and suitable for sustainable developmental applications. Understanding how temperature influences the composition and characteristics of resulting ash is vital for optimising its performance in these roles. Cocoa pod husk represent 70%–80% of the whole fruit (Mael, 2024). Cocoa Pod Husk Ash (CPHA) is derived from the combustion of Cocoa pod husks, an agricultural post-harvest waste often deposited in farmlands without proper waste management approach in place thereby constituting a challenge to the environment in Cocoa producing areas especially in southwestern Nigeria and other West

1Babatunde.olawuyi@covenantuniversity.edu.ng and babatunde@futminna.edu.ng
2 clinton.uzomapgs@stu.cu.edu.ng
3 Ignatius.omuh@covenantuniversity.edu.ng
4 nb.iheama@unizik.edu.ng

African countries. Audu and Mamman (2013) presented the report of incorporating CPHA at 0 to 1% binder content using 0.2% step intervals in concrete with reported increase in compressive strength up to 0.6% CPHA binder content. CPHA incorporation in the study also resulted in increased initial and final setting times of the cement paste; improved workability of concrete, decrease water absorption and drying shrinkage of cement. It was thereby suggested as water repellent admixture in concrete and plastering works (Audu *et al*., 2013). Admixture is employed to modify the properties of ordinary concrete for better performance and cost effectiveness in use (Shetty, 2005). These admixtures are of various kinds and are usually imported and expensive. Bowan (2021) studied CPHA as partial replacement of cement and it was reported to give medium workability for both 0.46 and 0.56 water/cement (w/(c+byproduct)) ratio concretes. The method of incineration and the burning temperature of the CPH and the influence on properties of resulting CPHA was however not discussed. These properties are known to be of major importance to the performance characteristics of any agricultural waste ashes. This paper thereby presents a report of a study aimed at systematic investigation of the influence of calcination temperature on the chemical composition of CPHA, highlighting the evolution of major mineral oxides and exploring the resulting implications for material performance. It is an extract from a study on performance assessment of CPHA as alternative binder in mortar and concrete. The specific objectives addressed in this study is the analysis of the mineral oxide composition and phase evolution of CPHA at different combustion temperatures

## LITERATURE REVIEW

Cocoa pod husk (CPH) is a post-harvest agricultural waste generated from the Cocoa (*Theobroma Cacao*) production process. The global Cocoa industry produces vast quantities of waste, including Cocoa pod husks, which are traditionally discarded or underutilised. However, the environmental challenges associated with agricultural waste necessitate innovative approaches to waste management and valorisation. The construction community industry is unrelenting in using waste or recycled materials in concrete production because of the emphasis placed on sustainable construction (Bowan and Lamina, 2022). Cocoa pod husk ash (CPHA), derived from the incineration of cocoa pod husks, has attracted attention due to its potential applications in agriculture, construction, and materials science. Furthermore, the presence of amorphous silica in agro-waste ashes can enhance its use in construction materials, where it can contribute to the pozzolanic properties of cement when used as a partial replacement for Portland cement in concrete production (Olawuyi, Joshua, Hassan, Enejiyon, and Egwuda, 2017). Post-harvest agricultural waste ashes such as rice husk ash, millet husk ash, cassava peel ash, etc. have shown promise in the construction industry, particularly in the production of cement and concrete. Studies have indicated that using agro-waste ashes as a supplementary cementing material can improve the mechanical properties of concrete while reducing the carbon footprint associated with traditional cement production (Olawuyi, Saka, Nduka and Babafemi, 2019; Nduka, Olawuyi, Fagbenle, and Fonteboa, 2022). The pozzolanic reaction of silica in the agro-waste contributes to the formation of additional calcium silicate hydrate (C-S-H), which enhances the strength and durability of concrete. Additionally, incorporating agro-waste into concrete mixtures can improve workability and reduce water absorption, making it a sustainable choice for construction, focused on eco-friendly practices (Olawuyi *et al*., 2017).

The potential for using CPHA in construction reflects a broader trend of utilising agricultural wastes in building materials, supporting circular economic principles. Given that it affects the final product's strength, durability, and performance, the oxide composition of cement is crucial. Optimising cement formulations for a range of construction applications is made easier with an understanding of these elements. The hydration process and the properties of cement are significantly influenced by the major oxides, which are $Fe_2O_3$, $SiO_2$, $Al_2O_3$, and CaO.

According to ASTM 618-2022, what make up a pozzolanic material (specifically fly ash) are the combination of the useful oxides ($SiO_2$+ $Al_2O_3$+ $Fe_2O_3$) which must be minimum 70% for Class N (i.e. raw or calcined natural Pozzolan) and Class F (i.e. fly ash typically produced from burning anthracite or bituminous coal) Pozzolan, but 50% minimum for Class C (i.e. fly ashes containing total calcium contents, expressed as calcium oxide (CaO), higher than 10 %.) Pozzolan (See Table 1 extracted from ASTM C618-2022).

Table 1: Summary of Chemical Requirements for Pozzolan

| Chemical Requirements | Class | | |
|---|---|---|---|
| | N | F | C |
| $SiO_2+Al_2O_3+Fe_2O_3$ minimum% | 70 | 70 | 50 |
| $SO_3$ maximum % | 4 | 5 | 5 |
| Moisture Content maximum% | 3 | 3 | 3 |
| Loss on Ignition (LOI) maximum % | 10 | 6[A] | 6 |

[A:] The use of Class F Pozzolan containing up to 12.0 % loss on ignition may be approved by the user if either acceptable performance records or laboratory test results are made available.

**Source: ASTM C618 – 2022**

The Loss on Ignition (LOI) of the Pozzolan is also a requirement for acceptance and is given by ASTM C618-2022 as 10% maximum for Class N Pozzolan but 6% maximum for Class F and C Pozzolan. The $SiO_2$ content is also important for good performance of a Pozzolan. BS EN 197-1- 2011 specifies a minimum $SiO_2$ content of 25% by mass for a material to be considered as a Pozzolan. The composition of PC, the material for which the Pozzolan is to serve as a replacement is also important for proper comparative assessment. Typical oxide composition of PC as found in Neville (2012) is hereby presented in Table 2.

Table 2: Typical Oxide Composition of PC

| Oxide | Composition (%) |
|---|---|
| Silica ($SiO_2$) | 20 |
| Alumina ($Al_2O_3$) | 6 |
| Ferric Oxide ($Fe_2O_3$) | 3 |
| Calcium oxide (CaO) | 63 |
| Magnesium oxide (MgO) | 1.5 |
| Sulphur trioxide ($SO_3$) | 2 |
| Potassium oxide ($K_2O$) & | 1 |
| Sodium oxide ($Na_2O$) | |
| Others | 1 |
| Loss of Ignition (LOI) | 2 |
| Insoluble residue | 0.5 |

Source: Neville, 2012

The primary oxides in PC are presented in Table 2 as Calcium Oxide (CaO – 63%), Silica ($SiO_2$ – 20%), Alumina ($Al_2O_3$ – 6%), and Iron Oxide ($Fe_2O_3$ – 3%), which together constitute about 70-80% of cement composition.

## Experimental Procedure

### Materials

The main material used for the study is Cocoa Pod Husk (CPH). Fresh samples of CPH were collected from a small farm in Ekiti State (See Plate 1).

Plate 1: Raw Cocoa Pod as obtained from the Farm

The sample was air- and sun-dried to remove residual moisture and impurities. The dried husks were then ground into smaller particles to enhance combustion efficiency.

### Methods

### Cocoa Pod Husk Ash Production

The prepared CPH samples were combusted in a furnace (Model No.TC512 (see Plate 2) situated at the Chemical Engineering Laboratory of Covenant University, Ota at five different temperatures levels (500 $^{o}$C ($F_1$), 550 $^{o}$C ($F_2$), 600 $^{o}$C ($F_3$), 650 $^{o}$C ($F_4$), 700 $^{o}$C ($F_5$), 750 $^{o}$C ($F_6$) and 800 $^{o}$C ($F_7$)) for 6 hours, ensuring complete thermal degradation (See Plate 3).

Plate 2: Electric Furnace Used

After cooling, the ash was collected, ground to a fine powder, and stored in a sealed polyethene bag before sending it to Laboratories for analysis (Plate 3).

(a)  (b) 

Plate 3: CPHA Samples (a) $F_3$ at 600 $^oC$; (b) $F_7$ at 800 $^oC$.

**Chemical Composition**

The chemical composition of CPHA was determined using the X-ray Diffraction (XRD), X-Ray Fluorescence (XRF) and Fourier Transmission Infra-Red (FTIR) analysis. The analysis focused on oxides commonly associated with pozzolanic and adsorptive properties: $CaCO_3$, CaO, MgO, for the XRD; $SiO_2$, $K_2O$, CaO, MgO, $Al_2O_3$, $Fe_2O_3$, and loss on ignition (LOI) for the XRF, while the FTIR was used to examine the phase evolutions in the resulting ashes. The XRD and XRF were conducted in Rolab Research and Diagnostic Laboratory in Ibadan, Oyo State, Nigeria, while the FTIR on the other hand was conducted at the Covenant University Central Instrumentation Research Facility (CUCIRF) Laboratory of Covenant University, Ota.

**X-Ray Fluorescent (XRF) Analysis**

XRF is a non-destructive analytical technique used to determine the elemental and oxide composition of solid materials. In the context of CPHA, it helps identify and quantify key inorganic oxides formed after thermal decomposition of the biomass. The XRF spectrometer is a notable X-ray instrument mostly deployed for the non-destructive chemical characterization of minerals, rocks, and fluids. It operates on the principles of wavelength-dispersive spectroscopy using electron microprobes. The CPHA samples were investigated using a wavelength-dispersive X-ray fluorescence spectrometer (Bruker AXS S4, explorer). The XRF was used to measure from Na11 to U92 in the atomic number order. The XRF of CPHA samples was carried out on the pelletized specimens using the total cement analyser apparatus to determine the materials' chemical and oxides compositions. The results of oxide composition were then tabulated and discussed using the provisions ASTM C618-2022 for proper interpretation and references.

**X-Ray Diffraction Analysis**

X-ray diffraction (XRD) is a multifaceted non-destructive analytical method employed to examine physical properties, including phase composition, crystal structure, and orientation of powder, solid, and liquid materials.

The Rigaku MiniFlex 600 XRD Diffractometer was powered, and on the panel, the voltage and current were set to 30 kV and 15 mA, respectively. The temperature was set at 21-23 $^oC$. The computer system was switched on, and the software of XRD, TUMI was double-clicked to run. The settings dialogue was clicked, and all the required settings of power and temperature were checked to correspond to those of the XRD. The analysed material was finely ground, homogenised, and the average bulk composition was determined. The powdered sample was prepared using the sample preparation block and compressed in the flat sample holder to create a flat, smooth surface, which was later mounted on the sample stage in the XRD cabinet. The sample was poured into the sample holder and then placed in the sample chamber column. Then the door was shut and confirmed from the computer. The sample was analysed using the reflection-transmission spinner stage using the Theta-Theta settings. Two-Theta starting position was 4 degrees and ends at 75 degrees with a two-theta step of 0.026261 at 8.67 seconds per step. Tube current was 40 mA, and the tension was 45 VA. A Programmable Divergent Slit was used with a 5 mm width mask, and the Gonio Scan was used. The intensity of diffracted X-rays is continuously recorded as the sample and detector rotate through their respective angles. A peak in intensity occurs when the mineral contains lattice planes with d-spacings appropriate to diffract X-rays at that value of $\theta$. Although each peak consists of two separate reflections ($K\alpha_1$ and $K\alpha_2$), at small values of $2\theta$, the

peak locations overlap with $K\alpha_2$ appearing as a hump on the side of $K\alpha_1$. Greater separation occurs at higher values of θ. Typically these combined peaks are treated as one. The 2λ position of the diffraction peak is typically measured as the centre of the peak at 80% peak height. Results were then presented as peak positions at 2θ and X-ray counts (intensity) in the form of a table or an x-y plot (shown in Figure 1). Intensity (I) was reported as peak height intensity, that intensity above background. The relative intensity is recorded as the ratio of the peak intensity to that of the most intense peak (relative intensity = I/I1 x 100).

### Fourier Transmission Infra-Red (FTIR) Spectroscopy

The FTIR analysis was performed to detect functional groups and organic compounds in the ash for the determination of the extent of decomposition and oxidation at varying temperatures.

The CPHA calcinated at varied temperatures was analysed using a Cary 630 FTIR/ATR spectrometer made by Agilent Technologies, Malaysia, as available at CUCIRF, Ota. The CPHA powdery samples were placed in the sample-holder and scanned from 4000 to 500 $cm^{-1}$ with 64 scans at a resolution of 4 $cm^{-1}$. Test results were then interpreted for categorisation of the phases observed using the work of Nandiyanto, Oktiani, and Ragadhita, (2019).

## RESULTS AND DISCUSSION

### Physical Observation

At lower burning temperatures (500 oC-550 oC i.e. specimen F1 and F2), the ash was dark grey in colour, reflecting incomplete carbon combustion. As the temperature increased (550 oC-650 0C i.e. F3 – F5) – Plate 3(a), the ash turned whitish grey, indicating reduction in carbon content and enhanced mineral concentration. At far higher temperatures (800 oC – F7), the sample turned greenish – Plate 3(b), an indication of possible over-burning, indicating change of phase from amorphous to a crystalline. This is agreement with Neville (2012).

### Chemical Analysis of CPHA

The results of experiments on chemical analysis are discussed in the following sub-sections.

### Oxide Composition at Different Temperature

The XRF analysis revealed significant composition variations with increasing temperatures.

The oxide composition of CPHA at different temperatures is summarized in the Table 3. The Table revealed CaO as the major compound in the resulting ashes ranging between 40 – 54% by mass of the total oxide composition of CPHA. This was however noted to increase as the temperature of burning increases going from 40.3% for $F_1$ burnt at 500 $^oC$ to the upper end content of 53.4% for $F_3$ burnt at 600 $^oC$ and 51.03% for $F_4$ burnt at 650 $^oC$; beyond which it decreased to 45.2% for $F_5$ burnt at the 700 $^oC$ but then gave fluctuating lower CaO values for $F_6$ burnt at 750 $^oC$ as 41.1% and 45.2% for $F_7$ burnt at 800 $^oC$. The $SiO_2$ content of the CPHA exhibited similar trend as that of CaO; having the lowest value of 15.4% for $F_1$ burnt at 500 $^oC$ but gradually increased up to a peak of 20.6% for $F_4$ burnt at 650 $^oC$ before the lower value of 17.8% for $F_5$ burnt at 700 $^oC$. The $SiO_2$ content then increased to 23% for $F_6$ burnt at 750 $^oC$ and slightly further increased to 23.8% for $F_8$ burnt at 800 $^oC$ revealed as the optimum. Therefore, 600 – 650 $^oC$ temperature range can be adjudged as the best burning temperatures. This is agreement with the submission in Neville (2012).

Table 3: Oxide Composition of CPHA

| Temperature ($^oC$) | $SiO_2$ | $Al_2O_3$ | $Fe_2O_3$ | CaO | MgO | $Na_2O$ | $SO_3$ | $K_2O$ | LOI | $SiO_2$+ $Al_2O_{3+}$ $Fe_2O_3$ |
|---|---|---|---|---|---|---|---|---|---|---|
| $500^0C$ ($F_1$) | 15.38 | 10.22 | 5.52 | 40.32 | 0.72 | 0.20 | 4.05 | 0.71 | 6.28 | 31.22 |
| $550^0C$ ($F_2$) | 15.76 | 12.45 | 6.36 | 45.70 | 0.78 | 4.22 | 5.23 | 0.11 | 6.55 | 34.57 |

| | | | | | | | | | | |
|---|---|---|---|---|---|---|---|---|---|---|
| $600^0$C ($F_3$) | 15.96 | 10.97 | 4.24 | 53.35 | 0.77 | 5.24 | 5.17 | 0.12 | 3.32 | 31.17 |
| $650^0$C ($F_4$) | 20.57 | 11.22 | 6.41 | 51.03 | 0.30 | 0.20 | 5.12 | 0.10 | 4.72 | 38.2 |
| $700^0$C ($F_5$) | 17.83 | 11.09 | 5.09 | 45.20 | 0.80 | 3.20 | 5.24 | 5.09 | 6.28 | 34.01 |
| $750^0$C ($F_6$) | 23.00 | 10.59 | 5.30 | 41.12 | 0.33 | 5.21 | 8.12 | 0.13 | 8.12 | 38.89 |
| $800^0$C ($F_7$) | 23.77 | 11.78 | 5.53 | 45.19 | 0.57 | 3.23 | 4.34 | 0.12 | 4.50 | 41.08 |

The LOI of the CPHA also fluctuates as the burning temperature varies, giving the lowest value of 3.32% for $F_3$ burnt at 600 $^o$C, followed by $F_4$ (burnt at 650 $^o$C), whose LOI is 4.72%. All the CPHA samples burnt at the varied temperatures, however, had LOI values below 10% which is the limit for Class N Pozzolan, but specimen $F_3$ (burnt at 600 $^o$C), $F_4$ (burnt at 650 $^o$C) and $F_7$ (burnt at 800 $^o$C) met the LOI requirement for Classes F and C Pozzolan classification of ASTM C618-2022.

The $Al_2O_3$ and $Fe_2O_3$ also, gave similar trends, with $Fe_2O_3$ having a definite peak of 6.41% at 650 $^o$C ($F_5$) but the $Al_2O_3$ had fluctuating LOI as temperature increased. The sum of useful oxides in the CPHA (i.e. $SiO_2$+$Al_2O_3$+$Fe_2O_3$) ranges between 31.2% to 41.1% which fell far below the 70% minimum requirement of ASTM C 618-2022 for Classes N & F Pozzolans and below the 50% minimum requirement for the Class C Pozzolan.

The composition of CPHA as observed can be compared to that of PC with CaO content (of 53.4%) at the optimum burning temperature of 600 $^o$C, being slightly lower than that of typical PC (of 64% as presented in Table 2). All the CPHA samples had $SiO_2$ content lower than the minimum (25%) specified by BS EN 197-1-2011. The $SiO_2$ content at 650 $^o$C of 20.6% is of similar value as found in the typical PC composition (20%) given by Neville (2012) as shown in see Table 1. The CPHA calcined at temperature range of 600 – 650 $^o$C will therefore need to be combined with another reactive Pozzolan of high $SiO_2$ content for best performance as alternative binder or SCM.

**X-Ray Diffraction**

The XRD Pattern for CPHA is as represented in Figure 1. According to the XRD pattern, the primary crystalline contributors in ash from cocoa pod husks are usually:

Potassium-containing salts (sulfates, carbonates, and chlorides) peak between 28 and 35 degrees Celsius. The strong peak of calcite ($CaCO_3$), which is frequently seen when carbonates persist or precipitate, is about 29.4°. If silica stays crystalline, quartz ($SiO_2$) peaks at 26.6°. Oxides (CaO, MgO) peak at a higher 2θ (≈37–43°) if carbonates break down when heated.

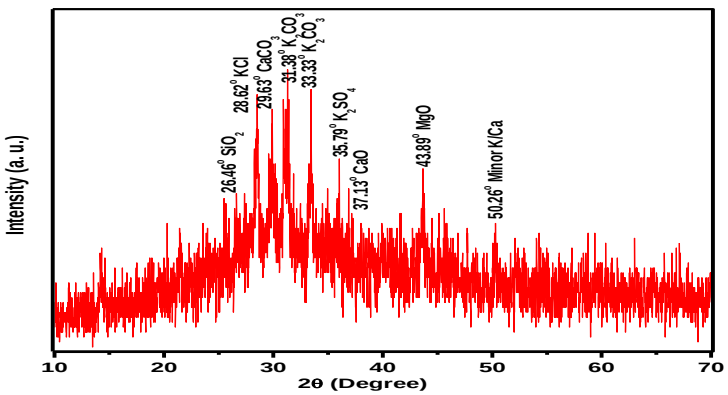


Figure 1: XRD Pattern for CPHA

Amorphous silica/glassy phases and carbonaceous leftovers produce a broad hump of about 15 to 30 degrees, which is a very common characteristic of ashes formed from plants.

**Fourier Transmission Infra-Red Spectroscopy**

The FTIR spectrographs for the various CPHA samples are as presented in Figures 2 to 8.

The spectrograph in Figure 1 ($F_1$) interpreted using the details provided in the works of Nandiyanto *et al*. (2019) reveals a spread region around 3300-3500 $cm^{-1}$ in $F_1$ sample which indicates O–H stretching (alcohols, phenols) or N–H stretching (amines, amides).

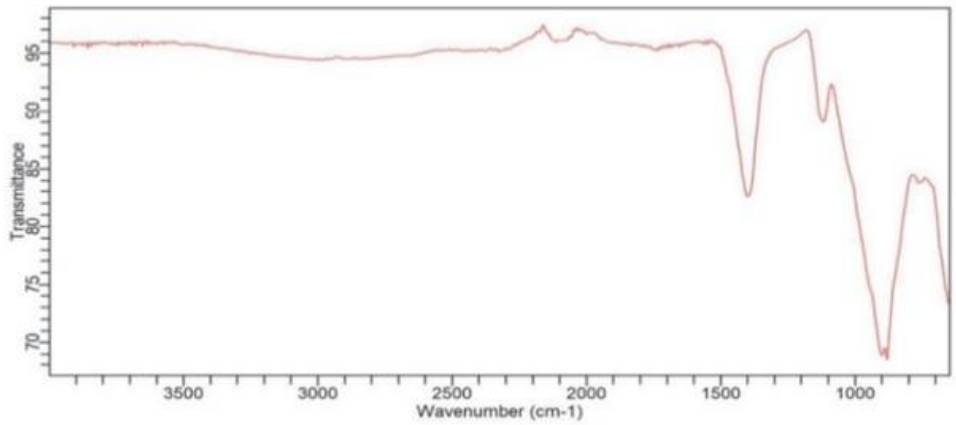


Figure 2: Spectrograph of Sample F1

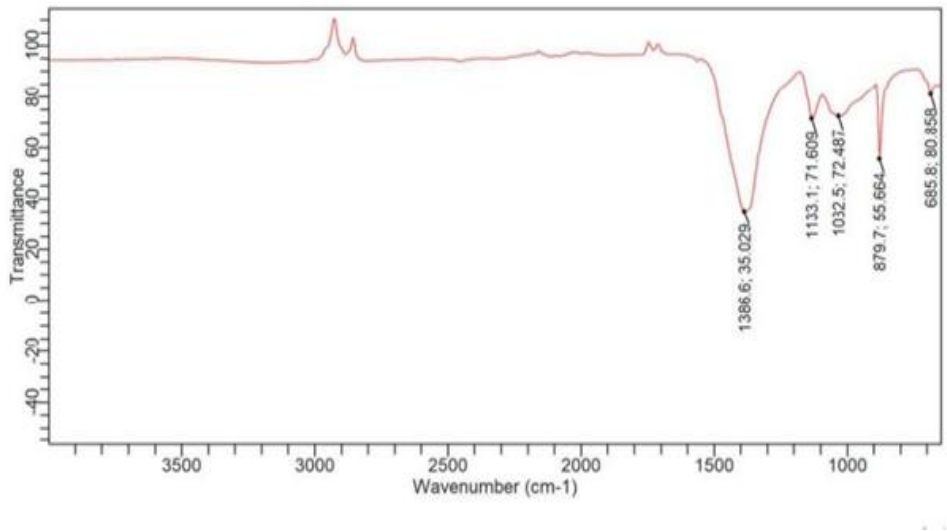


Figure 3: Spectrograph of Sample $F_2$

It also has a peak region of 2850–2950 $cm^{-1}$ representing C–H stretching vibrations of alkanes, with a small shoulder or weak peak suggesting aliphatic C–H groups. A strong peak around 1700 $cm^{-1}$ is likely due to a C=O (carbonyl) stretch, characteristic of ketones, aldehydes, carboxylic acids, or esters. 1600–1500 $cm^{-1}$ corresponds to C=C stretching in aromatics or N–H bending in amines. The region around 1250–1000 $cm^{-1}$ is characteristic of C–O stretching in alcohols, esters, or ethers. Strong peaks around 900–700 $cm^{-1}$ could be due to out-of-plane bending in aromatic compounds or C–H wagging.

The structure for $F_2$ sample in Figure 3 suggests an aromatic or unsaturated state, with strong peaks around 3000 $cm^{-1}$, C–O or C–N bonds, strong bending modes near 1133 and 1032 $cm^{-1}$, and bending peaks around 879 and 685 $cm^{-1}$

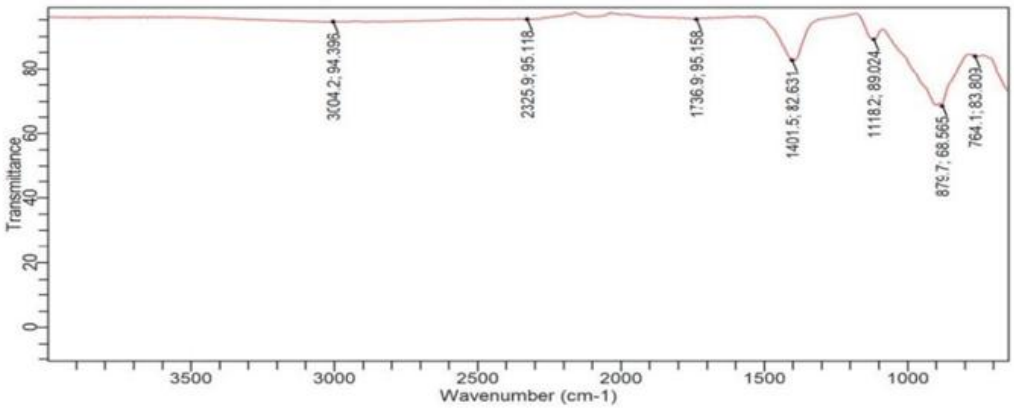


Figure 4: Spectrograph of Sample $F_3$

$F_3$ sample in Figure 4 indicates the presence of carbonyl groups, aromatic ring systems, and alkyl groups.

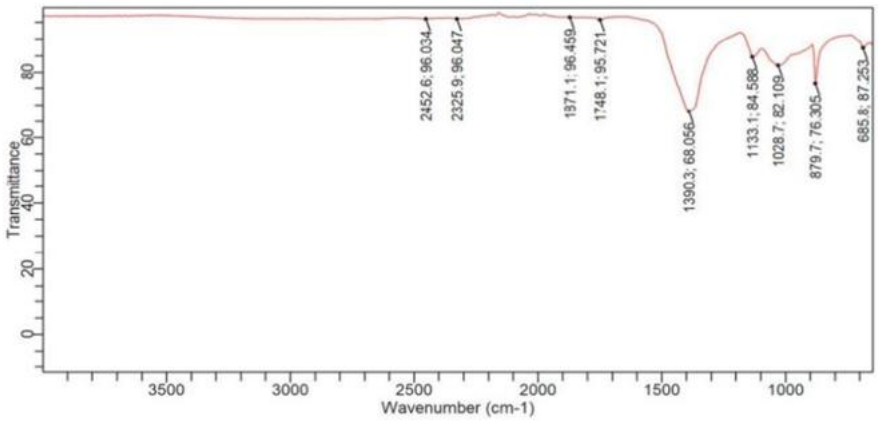


Figure 5: Spectrograph of Sample $F_4$

A strong peak at 1736 $cm^{-1}$ suggests an ester, while C–H stretches, and out-of-plane bends confirm the aromatic ring system. Alkyl groups show weak bending at around 1400 $cm^{-1}$.

The FTIR spectrum in Figure 4 reveals $F_4$ as a compound with a strong ester functional group, aromatic ring structure, and alkyl chains, suggesting a phthalate ester or similar aromatic polyester compound. The presence of an ester, a carbonyl group, a C-O stretch, an aromatic ring system, and alkyl groups, with the most likely ester being ether.

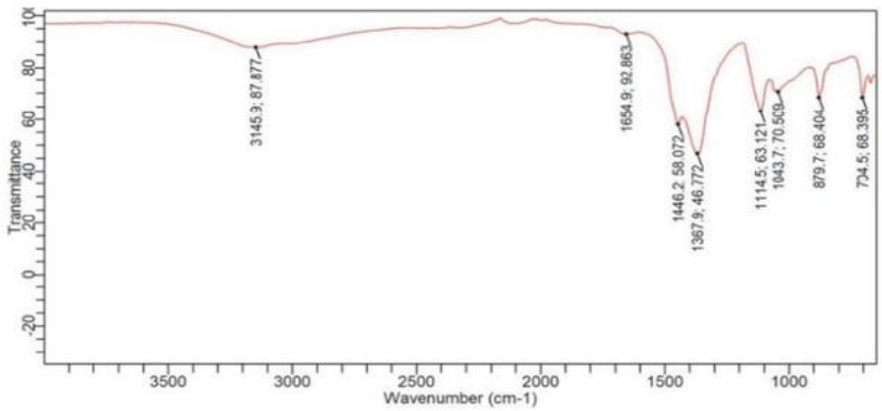


Figure 6: Spectrograph of Sample $F_5$

The $F_5$ sample as shown in Figure 6 contains an aromatic ring, an amino or hydroxyl group, C–O and $CH_2/CH_3$ groups and may be part of a functionalized aromatic compound or polymer additive. various chemical elements in a substance, including broad N–H/O–H stretch, C=O/C=C stretch, alkyl groups, C–O stretch, and aromatic C–H bending, which may indicate a secondary amine or hydroxyl group are identified.

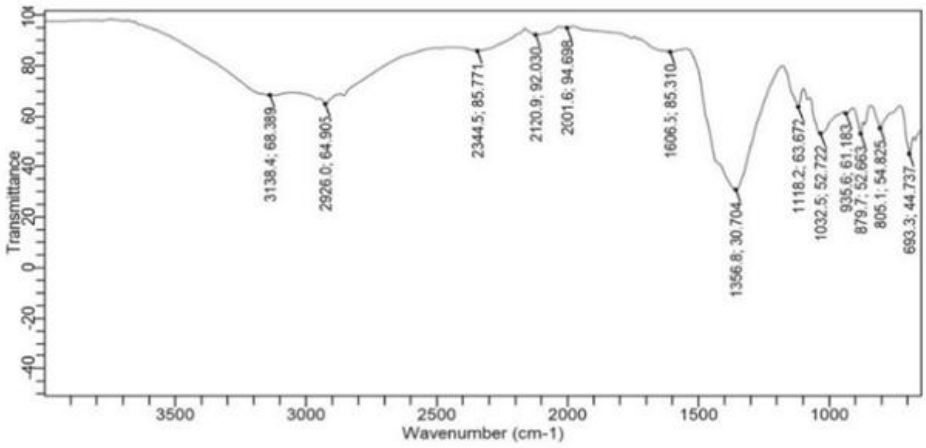


Figure 7: Spectrograph of Sample $F_6$

The main functional groups identified in $F_6$ sample (Figure 7) include an aromatic ring with bands at 1606, 897, 875, 867, and 693 $cm^{-1}$, a hydrogen or amine group with a broad peak at 3138 $cm^{-1}$, alkyl chains with C–H stretches around 2926 $cm^{-1}$, a weak to moderate C≡C or C≡N band at 2120 $cm^{-1}$, and C–O or C–N bands.

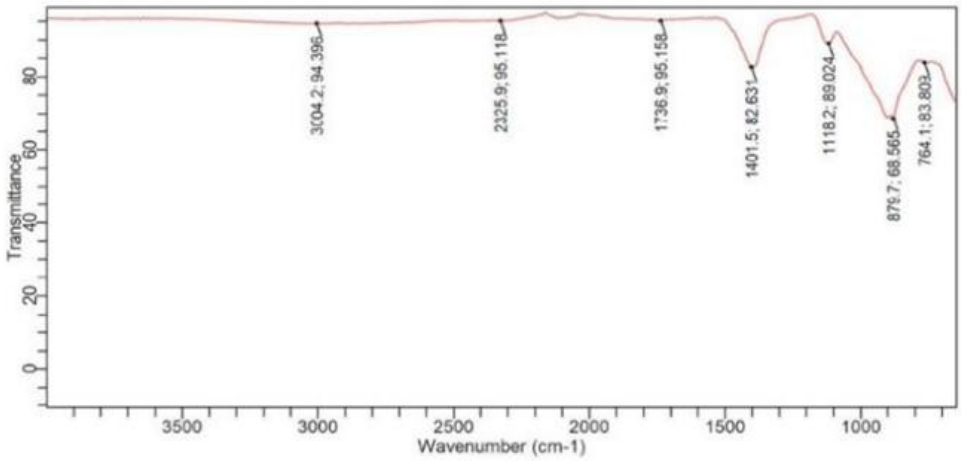


Figure 8: Spectrograph of Sample $F_7$

The spectrum in Figure 8 for $F_7$ sample indicates the presence of a carbonyl group, aromatic rings, ester or ester C-O bonds, weak but detectable free hydroxyl groups, and a possible alkene or amide component in the 1650 $cm^{-1}$ region.

## CONCLUSION AND RECOMMENDATION

### Conclusion

The study showed that temperature has a major impact on the mineralogical makeup and composition of the CPHA. Significant variation in the concentration of vital oxides like $SiO_2$+, Al2O3+Fe2O3 was observed as the burning temperature changed. The burning temperature range of 600 – 650 $^oC$ was found best for the CPHA to remain amorphous, while the CPHA sample burnt at this temperature range can be considered in combination

with a reactive Pozzolan of high silica content to serve as supplementary cementitious material in mortar and concrete.

**Recommendation**

The following recommendations are offered based on the findings of the study

i. Thermal treatment of Cocoa Pod Husk (CPH) should be carried out at moderate temperatures, ideally between 600°C and 650°C, to optimise the oxide composition and keep the resulting ash in the amorphous state.

ii. CPHA subjected to 600 – 650 $^{o}$C burning temperature should be used in combination with a reactive Pozzolan of high silica content to serve as supplementary cementitious material in mortar and concrete.

iii. Further study for evaluation of the strength activity index of CPHA in combination with a highly reactive Pozzolan, like rice husk ash, is recommended.

**Author's Contribution**

**B.J. Olawuyi** contributes to the conception, experimental work, analysis, manuscript writing, formatting and editing; **C.C. Uzoma** was involved in the conception, experimental work and manuscript writing; **I.O. Omuh** was involved in conception, manuscript writing, formatting and editing; while **N.B. Iheama** contributed to manuscript writing, formatting and editing.

## ACKNOWLEDGEMENT

The author(s) express their gratitude for assistance received from the Covenant University Centre for Research, Innovation, and Discovery (CUCRID); the Covenant University Central Instrumentation Research Facility (CUCIRF) Laboratory; the Department of Building Technology, and the University Management.

## REFERENCES

1. ASTM International (2022). ASTM C618: Specification Standards for Coal Fly Ash and Raw or Calcined Pozzolan for Use in Concrete. ASTM International, West Conshohocken, PA. Retrieved from www.astm.org.
2. Audu, V.E.M. and Mamman, Y.W. (2013). Use of Cocoa Pod Husk Ash as Admixture in Concrete, International Journal of Engineering Research and Technology (IJERT), 2 (11), ISSN: 2278-0181; https://doi.org/10.17577/IJERTV2IS110716
3. Awoyera, P. O. and Ugwu, E. I. (2022). Overview on environmental impact of recycled aggregate concrete incorporating pozzolans or fillers. In The Structural Integrity of Recycled Aggregate Concrete Produced with Fillers and Pozzolans (pp. 435-444). Woodhead Publishing.
4. Balador, Z. (2024). Agricultural by-products as construction materials. In Sustainability and toxicity of building materials (pp. 263-287). Woodhead Publishing.
5. Bowan P. A. and Limann H. (2022) Cocoa Pod Husk Ash as Partial Replacement of Cement in Concrete Production. Communication in applied science. Volume 10 (1).
6. Bowan, P.A. (2021). Cocoa Pod Husk Ash as Partial Replacement of Cement in Concrete Production, Communications in Applied Sciences, Infinity Press, 10 (1), ISSN 2201-7372.
7. British Standards Institution (2011). BS EN 197-1- Cement. Composition, Specifications and Conformity Criteria for Common Cements, Part 1. BSI, London.
8. Mael, S.H. (2024) Cocoa Pod Husk Meal as a Feed Ingredient for Livestock, **https://doi.org/10.1002/fes3.70003.**
9. Nandiyanto, A.B.D., Oktiani, R. and Ragadhita, R. (2019). How to Read and Interpret FTIR Spectroscope of Organic Material, Indonesia Journal of Science & Technology, 4 (1), 97-118.

10. Nduka, D.O., Olawuyi, B.J., Fagbenle, O.I. and Fonteboa, B.G. (2022); "Assessment of the Durability Dynamics of High-Performance Concrete Blended with a Fibrous Rice Husk Ash", Crystals, 12(1), 75; MPDI Publishing, https://doi.org/10.3390/cryst12010075.
11. Neville, A.M. (2012). Properties of Concrete (Fifth Ed.), Trans-Atlantic Publications, Inc.
12. Olawuyi, B.J., Joshua, O., Hassan, I.O., Enejiyon, M.O. and Egwuda, C.I. (2017). Exploratory Study on Agro-waste Ashes Combination with Industrial Waste as Alternative Binders in Concrete, Paper presented at 2017 Nigerian Building and Road Research Institute (NBRRI) International Conference on Emerging Materials & Technologies for Sustainable Building and Road Infrastructure, NAF Conference Centre, Abuja on 22nd – 24th June.
13. Olawuyi, B.J.**,** Saka, R.O., Nduka, D.O. and Babafemi, A.J. (2019). "Comparative Study of Superabsorbent Polymers and Pre-soaked Pumice as Internal Curing Agent in Rice Husk Ash Based High-performance Concrete", 3rd International Conference on Application of Superabsorbent Polymers and other New Admixtures towards Smart Cities, Skukuza, Kruger National Park, South Africa, 25th – 27th Nov. Published in RILEM Book Series 2020 (Chapter 9) by SpringerLinks.
14. Oyebisi, S., Igba, T., and Oniyide, D. (2019). Performance evaluation of cashew nutshell ash as a binder in concrete production. Case Studies in Construction Materials, 11, e00293.
15. Parlato, M. C. M., Valenti, F., Guerrini, L., Perbellini, A., and Pezzuolo, A. (2025). From agricultural by-products to building materials: A spatial modelling approach to foster green construction sector. Cleaner Environmental Systems, 100307.
16. Sarangi, S. and Suganya, O. M. (2024). A comprehensive review of the physical and mechanical characteristics of agricultural by-products as cementitious alternatives in the production of sustainable concrete. Materials Today Sustainability, 27, 100882.
17. Kumar, R., and Kapur, A., (2025), Sustainable building materials: a pathway to sustainable development. Journal of civil Engineering 23(5):172-187.